ANTIOXIDANTS & REDOX SIGNALING
Volume 9, Number 12, 2007

DOI: 10.1089/ars.2007.1786

Forum Original Research Communication

Hippocampal Cellular Stress Responses After Global Brain Ischemia and Reperfusion

GEORGE G. ROBERTS,[1] MIKE J. DI LORETO,[1] MONIQUE MARSHALL,[1]
JIE WANG,[1] and DONALD J. DEGRACIA[1,2]

ABSTRACT

Brain ischemia and reperfusion (I/R) induce neuronal intracellular stress responses, including the heat-shock response (HSR) and the unfolded protein response (UPR), but the roles of each in neuronal survival or death are not well understood. We assessed the relative expression of UPR (ATF4, CHOP, GRP78, XBP-1) and HSR-related (HSP70 and HSC70) mRNAs and proteins after brain I/R. We evaluated these in hippocampal CA1 and CA3 after normothermic, transient global forebrain ischemia and up to 42 h of reperfusion. In CA1, *chop* and *xbp-1* mRNA showed maximal 14- and 12-fold increases, and the only protein increase observed was for 30-kDa XBP-1. CA3 showed induction of only *xbp-1*. GRP78 protein declined in CA1, but increased twofold and then declined in CA3. Transcription of *hsp70* was an order of magnitude greater than that of any UPR-induced transcript in either CA1 or CA3. HSP70 translation in CA1 lagged CA3 by ~24 h. We conclude that (a) in terms of functional end products, the ER stress response after brain ischemia and reperfusion more closely resembles the integrated stress response than the UPR; and (b) the HSR leads to quantitatively greater mRNA production in postischemic neurons, suggesting that cytoplasmic stress predominates over ER stress in reperfused neurons. *Antioxid. Redox Signal.* 9, 2265–2275.

INTRODUCTION

Brain ischemia and reperfusion (I/R) are associated with a profound inhibition of protein synthesis, the lack of recovery from which correlates with delayed neuronal death (DND) (14). Hence, much interest exists in ascertaining the mechanisms of I/R-induced translation arrest and its contribution to cell death (reviewed in 5, 6, 14, and 36). It has recently been argued that postischemic translation arrest is intimately involved with the neuronal intracellular stress responses after I/R injury (6).

It has been well established for more than two decades that brain I/R strongly activates the heat-shock response (HSR), particularly transcription of the 70-kDa inducible heat-shock protein (HSP70) (reviewed in 38). Expression of the HSR distinguishes vulnerable from resistant brain regions, but expression patterns are complex, and the significance of this complexity is not presently understood (41). An increasing number of reports assess the endoplasmic reticulum (ER) stress response, the unfolded protein response (UPR), after brain I/R. However, expression of the UPR in reperfused brain does not exactly parallel that which occurs *via* pharmacologic manipulation of cell-culture systems (reviewed in 6, 7), and it is unclear presently if brain I/R induces a classic UPR, by which is meant the simultaneous activation of the PERK, IRE1, and ATF6 pathways.

Although the degree to which brain I/R induces the UPR requires clarification, it is also important to assess the relative contributions of the various intracellular stress responses toward enhancing or preventing DND. To approach this issue adequately, knowledge of the relative magnitudes and regional localization of neuronal intracellular stress responses is required.

[1]Department of Physiology and [2]Center for Molecular Medicine and Genetics, Wayne State University School of Medicine, Detroit, Michigan.

Recent studies suggest that HSR induction, as measured by *hsp70* transcription, is substantially greater than the UPR, as measured by *grp78* transcription (23, 34).

We further investigated the differential expression of HSR and UPR markers in vulnerable and resistant hippocampal regions after brain I/R. We observed that vulnerable CA1 generally displayed a greater magnitude of stress gene expression for both the HSR and for some UPR-associated genes, as compared with CA3. However, the profile of UPR-associated gene expression did not resemble a classic UPR, which, for example, is characterized by increased transcription of *chop* and *grp78* (19). Instead, ER stress–associated gene expression more resembled the integrated stress response (ISR), a transcriptional program activated by phosphorylation of the alpha subunit of eukaryotic initiation factor 2 (eIF2α) (39). Additionally, expression of the HSR in both CA1 and CA3 was at least an order of magnitude greater than any UPR/ISR-associated gene.

MATERIALS AND METHODS

Materials

ATF6 antiserum (IMG-273) was purchased from Imgenex (San Diego, CA). Antiserum specific for phosphorylated eIF2α [eIF2α(P); 44-728G] was purchased from Biosource International (Camarillo, CA). ATF4 (sc-200), GAPDH (sc-25778), and CHOP (GADD153, sc-575) antisera were purchased from Santa Cruz Biotech (Santa Cruz, CA). GRP78 antiserum (645-354) was purchased from Calbiochem (Darmstadt, Germany). Antiserum for HSP70 (SPA-812) and pure recombinant HSP70 (SPP-758) protein were purchased from Cell Signaling Technologies (Danvers, MA). Antiserum for XBP-1 was a kind gift of Drs. Heather Harding and David Ron (Skirball Institute, New York University School of Medicine). Thapsigargin (T9033) and protease inhibitor cocktail (P8340) were purchased from Sigma Chemical Co. (St. Louis, MO). All other chemicals were reagent grade.

Brain ischemia and reperfusion model

All animal experiments were approved by the Wayne State University Animal Investigation Committee and were conducted by following the *Guide for the Care and Use of Laboratory Animals* (National Research Council, revised 1996). All efforts were made to reduce animal suffering and minimize the total number of animals used. Global forebrain ischemia was induced by using the bilateral carotid artery occlusion and hypovolemic hypotension (2VO/HT) model of Smith *et al.* (42). Male Long Evan rats (275–300 g) were initially anesthetized with 5% halothane, and anesthesia was maintained at 2% halothane in 100% O_2 by using a face mask through the duration of the experiment. Rectal temperature was maintained at 37 ± 0.5°C by a homeostatic blanket system (Harvard Apparatus) during ischemia and for the first 1 h of reperfusion. Mean arterial pressure (MAP) was monitored in real time *via* tail artery access. The common carotids were isolated and lassoed bilaterally. Blood gas measurements ensured a pH of 7.4 ± 0.1, pO_2 >80 mm Hg, and pcO_2 of 35 ± 5 mm Hg immediately before the initiation of ischemia. Blood was withdrawn, *via* femoral arterial access, into a 10-ml syringe to a MAP of 50 mm Hg, and carotids clamped by using microaneurysm clips. Blood was further withdrawn to maintain the MAP at 40 mm Hg for the 10-min duration of ischemia. After ischemia, blood was reinfused at a rate of 5 ml/min. All cutdown wounds were sutured, and anesthesia and temperature control were maintained for 1 h after surgery. Postsurgical animals were housed in a 12-h light/dark cycle and provided food and water access during the reperfusion period. Animals displaying frank necrosis, weight loss >15% initial body weight/day, or sustained seizure activity were excluded from the study.

Experimental groups and the respective sample number, *n*, are indicated as appropriate in the following sections. Nonischemic controls (NICs) were sham operated but did not receive carotid clamping and blood withdrawal. For all reperfusion groups, 10-min 2VO/HT was used unless otherwise stated. Reperfusion durations ranged from 10 min to 72 h, and all reperfusion groups, except the 10-min group (10mR) are designated by the number of hours followed by an "R" (*e.g.*, 72-h reperfusion is 72R).

Perfusion fixation and general cell staining

Nonischemic controls (NICs), or rats subjected to 10-min ischemia and either 24 h (24R), 48 h (48R), or 72 h (72R) ($n = 3$ per group) were transcardially perfused with 40 ml of 0.9% NaCl solution followed by 300 ml of 4% paraformaldehyde (PFA) in 0.1 *M* PBS solution at a flow rate of 20 ml/min. Brains were postfixed overnight by immersion in 4% PFA/0.1 *M* PBS. Fifty-micrometer slices through the dorsal hippocampus were obtained with a vibratome and stored at −20°C in cryostat solution until used. For toluidine blue staining, slide-mounted slices were washed thrice in 1× PBS and air-dried overnight. Sections were dehydrated in a graded ethanol series and then incubated in a 10% toluidine blue in 100% ethanol solution for 1 h at room temperature. Slides were washed in a graded ethanol series followed by 100% xylene. Slides were then coverslipped with Permount and viewed under wide-field visible light microscopy.

Hippocampal homogenates

After the respective durations of reperfusion, animals were killed with 5% halothane, decapitated, and the hippocampi rapidly dissected on a precooled dissecting microscope stage. Whole hippocampi were removed bilaterally, pooled from the same animal, and sonicated at 1:10 wet wt/vol in buffer A (1% Triton X-100, 50 m*M* HEPES, pH 7.4, 10% glycerol, 150 m*M* NaCl, 1 m*M* EDTA, 100 m*M* NaF, 25 m*M* DTT, 25 m*M* sodium orthovanadate, 13 m*M* β-glycerophosphate, 10 m*M* tetrasodium pyrophosphate, and 1:85 dilution of protease inhibitor cocktail). Unfractionated whole hippocampal homogenates were analyzed with Western blot as described later.

Microdissection of CA1 and CA3

After the respective durations of reperfusion, animals were killed with 5% halothane, decapitated, and brains rapidly but carefully dissected. Whole brains were snap frozen in dry ice and ethanol for 15 sec. Hippocampal CA1 and CA3 were then dissected under a dissecting microscope from semifrozen slices

obtained from a coronal section of the semifrozen brain cut approximately −2.30 to −3.80 mm posterior to bregma (37). The CA3 region was separated by a vertical cut slightly medial to the curve of the CA3, followed by a second vertical cut at the lateral edge of the dorsal hippocampus. Surrounding cortex was removed to provide isolated CA3. The CA1 region was separated from the DG by a roughly horizontal cut passing through the obliterated hippocampal fissure, which is delineated by a continuous line of large, cross-sectioned blood vessels. The corpus callosum on the superior surface was removed to complete the isolation of CA1. The resulting dissections were weighed, hand-homogenized on ice in buffer A at 1:10 wet wt/vol, and Western blots were as described later. For a single rat, pooled, bilateral dissections of CA1 or CA3 gave 3–7 mg wet weight per each region.

Real-time PCR

Real-time PCR was performed as previously described (28). Total nucleic acids were purified by hot phenol extraction (31). In brief, microdissected CA1 and CA3 were placed in 1 ml of buffer prewarmed to 65°C containing 25 m*M* Tris pH 8.0, 10 m*M* EDTA, 100 m*M* NaCl, 1 m*M* EDTA to which 0.5% SDS was added after autoclave sterilization, and 500 μl phenol prewarmed to 65°C and hand-homogenized in a Dounce homogenizer. The upper phase was further phenol extracted 4 times, followed by two chloroform extractions.

RNA was isolated from total nucleic acid preparations by addition of 2 units of RQ1 RNase-free DNase I (Promega Biotech, Madison, WI) per microgram of nucleic acids determined by absorbance at 260 nanometers. DNase reactions were incubated at 37°C for 30 min, followed immediately by phenol/chloroform extraction and precipitation in ethanol to destroy further DNase activity. Total RNA was primed with random hexamers (Invitrogen, Carlsbad, CA) and reverse transcribed by using the SuperScript II enzyme from Invitrogen. The resulting cDNA was used as template for real-time PCR with the ABI Prism 7700 Sequence Detection System (ABI, Foster City, CA) according to manufacturer's instructions. Primer sequences used to quantitate levels of *chop, gapdh, grp78, hsc70, hsp70,* and *xbp-1* are listed in Table 1. Relative transcript levels were determined by using the $\Delta\Delta C_T$ method (25), with *gapdh* as internal control, and NIC levels set at 1.0. Transcript levels in CA1 and CA3 reperfusion groups were determined from three separate animals per group, expressed as fold over NIC values, averages taken, and groups compared with one-way ANOVA, and Tukey *post hoc* testing where appropriate.

Western blotting

Homogenate protein concentrations were determined by using the Folin phenol method. For whole hippocampal homogenates and microdissected homogenates, 125 and 50 μg protein/lane, respectively, were run on 10% SDS-PAGE gels and then electroblot transferred to nitrocellulose (Schleicher and Schuell, BA85, 0.45 μm). Western blots were performed as previously described (8), and primary antisera dilutions were ATF4 (1:400); ATF6 (1:250); CHOP (1:400); eIF2α(P) (1:750); GAPDH (1:1,000); HSP70 (1:500); and XBP-1 (1:1,000). Immunoblots were analyzed with scanning densitometry (Intelligent Quantifier, ver. 4.0; BioImage, Jackson, MI). Experimental groups were compared with one-way ANOVA followed by Tukey *post hoc* testing if appropriate.

TABLE 1. PRIMER SEQUENCES USED FOR REAL-TIME PCR

Gene	*Primer sequence*
CHOP (43)	5′-GCACCTCCCAAAGCCCTCGC-3′
	5′-CCGTTTCCTAGTTCTTCCTT-3′
GAPDH	5′-TCCCATTCTTCCACCTTTGA-3′
	5′-CATGTAGGCCATGAGGTCCACCAC-3′
GRP78 (4)	5′-CCACCAGGATGCAGACATTG-3′
	5′-AGGGCCTCCACTTCCATAGA-3′
HSC70	5′-GCAACCCTATCATCACCAAG-3′
	5′-GGCCTGAAGAAGCACCACCA-3′
HSP70 (26)	5′-TTCGTGGAGGAGTTCAAGAG-3′
	5′-AGAGTCGATCTCCAGGC-3′
XBP-1	5′GGATTCTGACGCTGTTGCCT-3′
	5′-AGGGAGGCTGGTAAGGAACT-3′

Sequences taken from other studies show references.

Cell-culture studies

Neuroblastoma 104 cells were neuronally differentiated and treated with 2 μ*M* thapsigargin (an inducer of ER stress), for 3 h, as previously described (21). For Western blotting, cells were lysed in the homogenization buffer and treated identically to brain homogenates, as described earlier. For RT-PCR studies, cells were scraped, pelleted at 4°C, 500 *g*, for 5 min, and then lysed by the hot phenol method described earlier, and the primers listed in Table 1 used for RT-PCR, as described.

RESULTS

Cell death in CA1

Validation that the 2VO/HT model produced CA1 pyramidal cell death at 72-h reperfusion (72R) was performed by staining with Toluidine blue. At 72R, after 10-min 2VO/HT, the CA1 pyramidal neurons were dead (Fig. 1B and 1D), and no detectable loss of neurons in CA3 was seen (Fig. 1C). Massive shrinkage of 3DR CA1 pyramidal neurons with pycnotic nuclei was found, with occasional preservation of CA1 pyramidal layer interneurons, and invasion of the CA1 layer by activated microglia (Fig. 1D, arrow). In other published work, we did not observe loss of neurons in hippocampal dentate gyrus or cortical layers II/III, V, or VI, nor did we observe hippocampal cell loss at 24 or 48 h of reperfusion, as determined by FluoroJade staining (8). Thus, as is well established (42), the 2VO/HT model produced the expected pattern of CA1 cell death.

The UPR and HSR in whole, unfractionated hippocampus

We evaluated protein markers of the HSR and UPR in unfractionated hippocampus. Figure 2A evaluated eIF2α phosphorylation at 10-min (10mR), 90-min (1.5R) and 4-h (4R) reperfusion after 10-min 2VO/HT, and the densitometry is

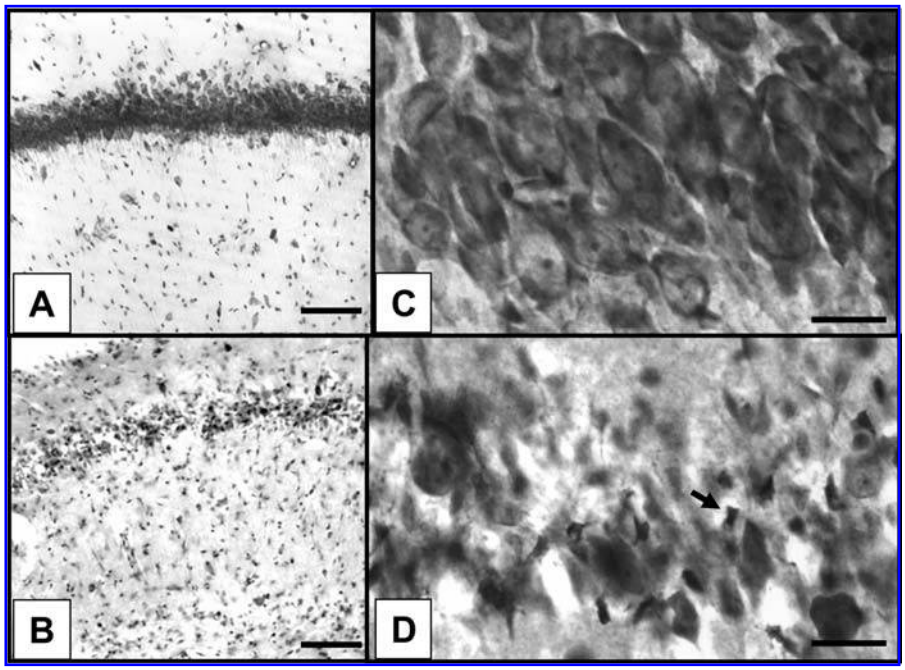

FIG. 1. Assessment of neuronal death after brain ischemia and reperfusion. Low-power images of toluidine blue staining of (**A**) nonischemic control hippocampal CA1, and (**B**) hippocampal CA1 after 10-min ischemia and 72-h reperfusion. Higher-power micrographs at 72-h reperfusion, after 10-min ischemia for (**C**) CA3 and (**D**) CA1. The 10-min ischemia and 72-h reperfusion led to the selective death of only CA1 neurons. *Arrow* in **D**, an activated microglia, which can be seen invading the CA1 pyramidal cell layer. Scale bars in **A** and **B** are 250 μm, and in **C** and **D** are 20 μm.

shown in Fig. 2C. Phosphorylation of eIF2α showed a maximal increase over NICs of fivefold at 10mR. We also evaluated CHOP, XBP-1, and ATF4 at these time points, but observed no increase in any of these proteins (data not shown).

We next evaluated the effect of ischemia duration on these same markers. Shown in Fig. 2B, at 24-h reperfusion (24R) after either 10-, 15-, or 20-min 2VO/HT ischemia, levels of eIF2α were indistinguishable from NICs, and no increase was noted

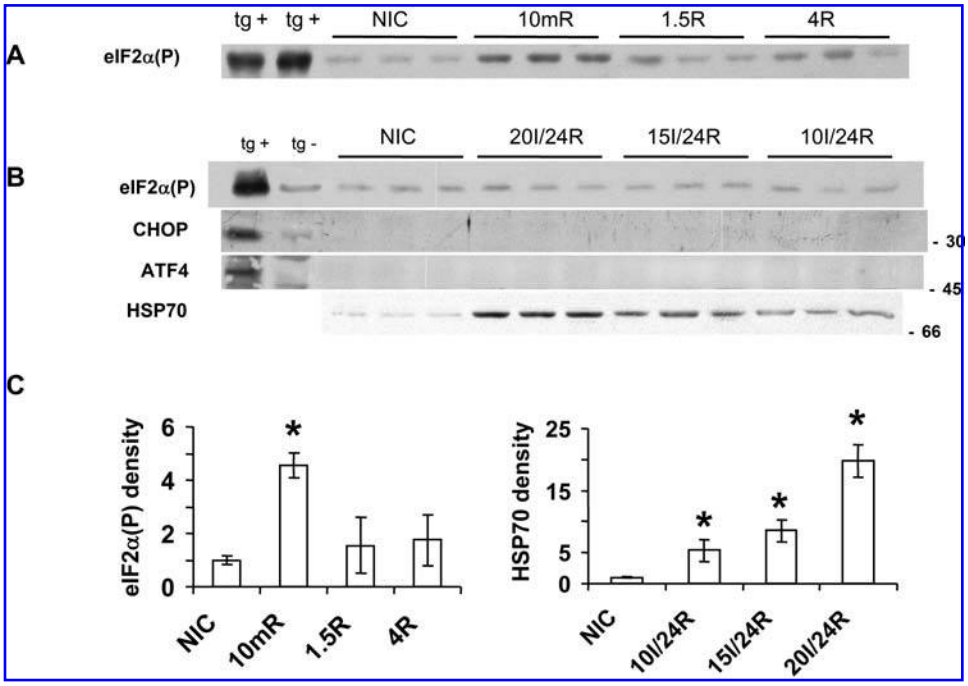

FIG. 2. Western blot detection of expression of cellular stress responses in whole, unfractionated hippocampus. (**A**) Western blot of eIF2α(P) at 10-min (10mR), 90-min (1.5R), and 4-h (4R) reperfusion. (**B**) Western blots for eIF2α(P), CHOP, ATF4, and HSP70 at 24-h reperfusion after either 10-min (10I/24R), 15-min (15I/24R), or 20-min (20I/24R) ischemia. (**C**) Densitometry of the eIF2α(P) blot in **A** (left) and the HSP70 blot in **B** (right). *Tukey *post hoc* $p < 0.05$ compared with NIC. Three animals were in each experimental group, as shown. Control lanes include NB104 cells either treated (tg+) or untreated (tg-) with thapsigargin. Molecular weight markers are indicated to the left of the blots in **B**.

in either CHOP or ATF4. In contrast, levels of HSP70 in unfractionated hippocampus at 24R were proportional to the duration of ischemia, with longer ischemia causing a greater increase in HSP70 production (Fig. 2C, graph).

UPR and HSR transcription in CA1 and CA3 after brain I/R

RT-PCR of transcripts induced by the UPR (*chop*, *grp78*, and *xbp-1*) and the HSR (*hsp70* and *hsc70*) were evaluated separately in microdissected CA1 and CA3 at reperfusion durations ranging from 8 to 42 h (Fig. 3A–E). We assessed to 42h to evaluate the lead-up to cell death in CA1, but to avoid later time points that may include dead CA1 cells. In nonischemic controls, mRNA expression ratios in CA1 compared with CA3 of *grp78*, *hsc70*, *hsp70*, *chop,* and *xbp-1* were in each case indistinguishable from unity (data not shown).

Transcription of *chop* in CA1 gradually increased and peaked at 12-fold over NIC at 30R (Fig. 3A), consistent with previous reports of CHOP transcription in unfractionated hippocampus (35, 43), but decreased to NIC levels at 42R. CA3 showed no change in *chop* transcription. We saw a trend of a fourfold increase in *grp78* transcription in CA1 (Fig. 3B), but because of a wide variance, this did not clear statistically. Less variance of *grp78* mRNA was noted in CA3, and the values were indistinguishable from NICs through reperfusion. Transcription

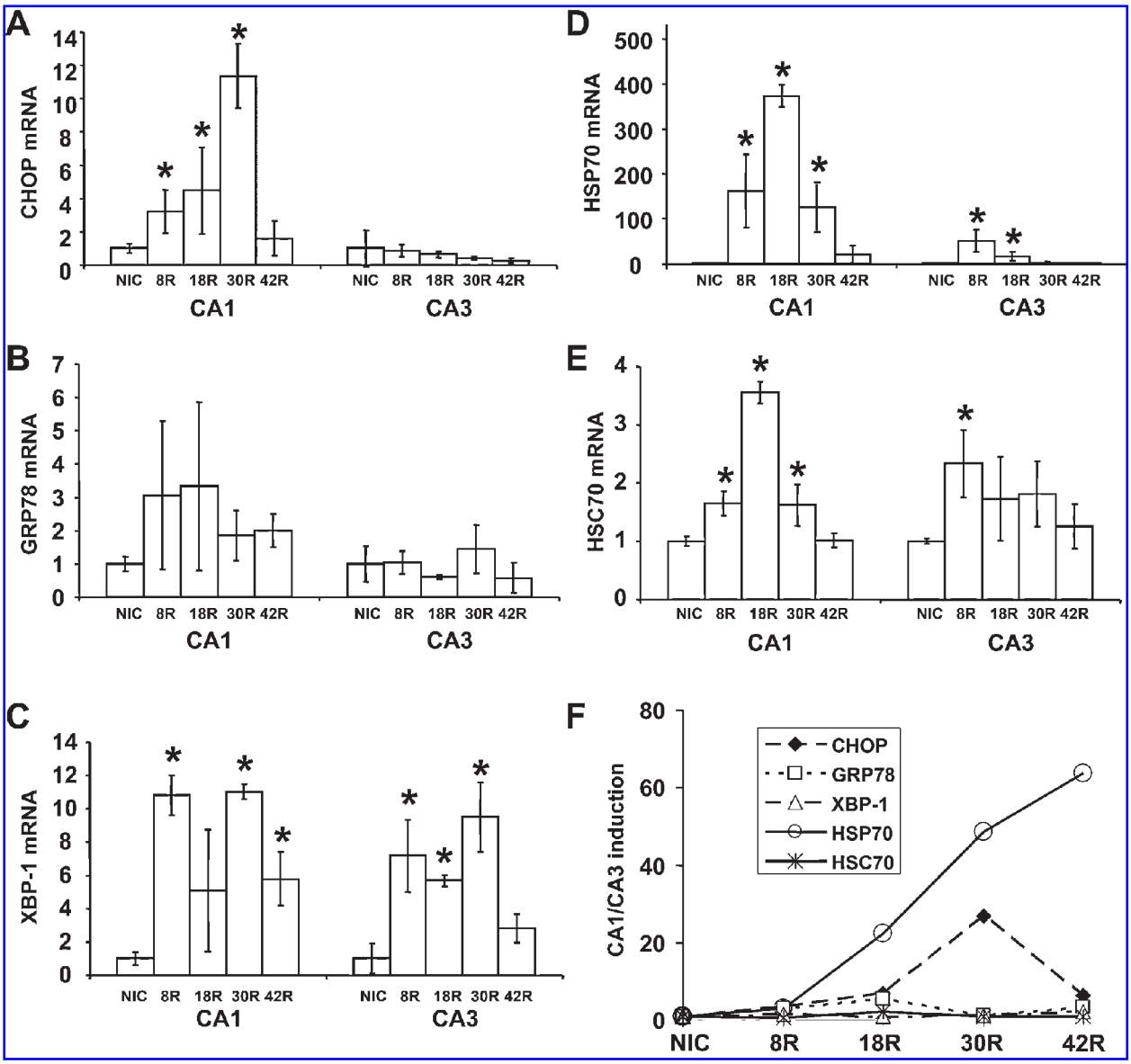

FIG. 3. Real-time PCR of UPR and HSR genes in microdissected hippocampal CA1 and CA3 as follows: (A) *chop*, (B) *grp78*, (C) *xbp-1*, (D) *hsp70*, and (E) *hsc70*. Primers used for RT-PCR are listed in Table 1. Graphs in **A–D**, fold increase over nonischemic controls, which were set to 1.0. *Tukey *post hoc* $p < 0.05$ compared with NIC. Three to five animals were in each experimental group. (**F**) Graph of the ratio of increase of each mRNA in CA1 divided by the increase in CA3. The reader is cautioned to note the different scales of the Y-axis for each graph.

of *xbp-1* occurred in both CA1 and CA3 (Fig. 3C), peaking at ~8- to 10-fold in both regions between 8R and 30R. At 42R, *xbp-1* transcripts were indistinguishable from controls in CA3, but remained about sixfold over controls in CA1.

We observed very large increases in *hsp70* transcription in both CA1 and CA3 (Fig. 3D). In both regions, *hsp70* levels were very high at 8R, increasing 160- and 50-fold in CA1 and CA3, respectively. The 8R value was the peak value for CA3, but CA1 showed a peak increase of ~375-fold over control at 18R. By 30R, levels of *hsp70* returned to controls in CA3, but remained high in CA1 at 126-fold control. By 42R, levels of *hsp70* in CA1 were still high at 20-fold control, greater than any UPR-induced transcript, but large interanimal variability prevented this value from clearing statistically compared with controls. We observed relatively small increases in transcription of the mRNA coding for the constitutive 70-kDa heat-shock protein, HSC70 (Fig. 3E). Levels of *hsc70* transcript peaked at 3.5-fold controls at 18R in CA1 and were 65% greater than controls at 8R and 30R. In CA3, *hsc70* approximately doubled at 8R, but we could not detect a difference from controls at later time points.

To visualize the relative transcriptional induction between CA1 and CA3, the ratio $\frac{(CA1_{REP}/CA1_{NIC})}{(CA3_{REP}/CA3_{NIC})}$ for each of the five transcripts was plotted as a function of reperfusion duration in Fig. 3F. For *grp78*, *xbp-1,* and *hsc70,* this ratio was relatively constant around unity in both regions. Transcription of *hsp70* in CA1 showed a continuous increase compared with CA3. Induction of *hsp70* in CA1 was about 60-fold higher than CA3 at 42R. For *chop*, this ratio was ~20 at 30R in CA1 compared with CA3, but approached unity at 42R.

Thus, although both CA1 and CA3 showed equivalent induction of *xbp-1*, neither showed significant induction of *grp78*, and only CA1 showed evidence of *chop* induction. Both regions showed very large increases in *hsp70* induction, but only a minor increase in the relative level of *hsc70.*

Translation of stress proteins in CA1 and CA3

For GRP78 in CA1, we detected a continuous decrease starting at 18R and continuing to about 25% of control values at 42R (Fig. 4). GRP78 increased twofold in CA3 by 18R, but declined thereafter, and was ~33% of control values at 42R. We could not detect the presence of CHOP or 55-kDa XBP-1, or an increase in 50-kDa ATF6 in either CA1 or CA3 at any time point tested (data not shown).

Translation of HSP70 in CA1 lagged CA3 by approximately 24 h (Fig. 5). In CA1, HSP70 was barely detectable at 8R and 18R, but these time points were the peak of HSP70 translation in CA3 (Fig. 5B). At 30R and 42R, HSP70 in CA1 continued to increase to levels higher than that observed at any time point in CA3. The levels of HSP70 consecutively decreased at 30R and 42R in CA3

The UPR and HSR in thapsigargin-treated NB104 cells

Transcription and translation of markers of the UPR and HSR in neuronally differentiated NB104 cells treated with thapsigargin (tg+) are shown in Fig. 6. Although transcription of *xbp-1*, *hsc70,* and *hsp70* (Fig. 6A) were similar to what was observed in reperfused brain, *chop* transcription was about 4 times

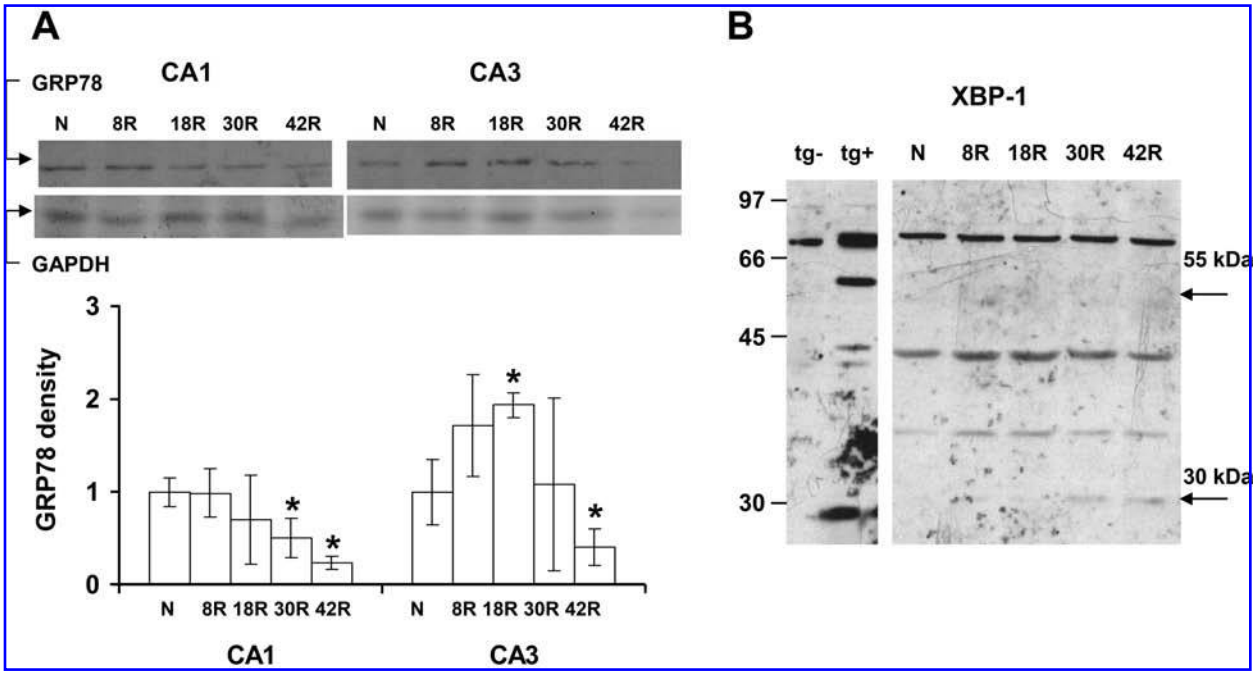

FIG. 4. (A) Western blots of GRP78 and GAPDH in representative samples of microdissected CA1 and CA3. (**B**) Densitometry of GRP78 normalized to GAPDH. Four animals were in each experimental group. N, nonischemic control (NIC); 8R, 18R, 30R, and 42R, 8-, 18-, 30-, and 42-h reperfusion after 10-min transient global forebrain ischemia. *Tukey *post hoc* $p <$ 0.05 compared with NIC.

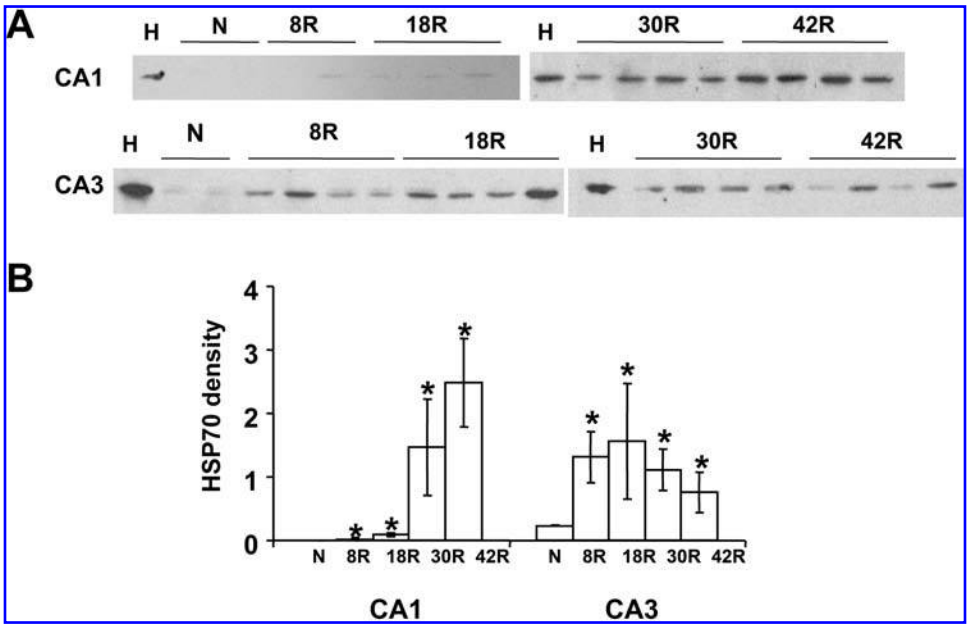

FIG. 5. (A) Western blots of HSP70 in microdissected CA1 and CA3, as labeled (abbreviations as in Fig. 4, except H, which is pure recombinant HSP70). (**B**) Densitometry of HSP70 normalized to GAPDH (GAPDH not shown). *Tukey *post hoc* $p < 0.05$ compared with NIC. Four animals were in each experimental group, although only two of the NICs are shown on the gels in **A**.

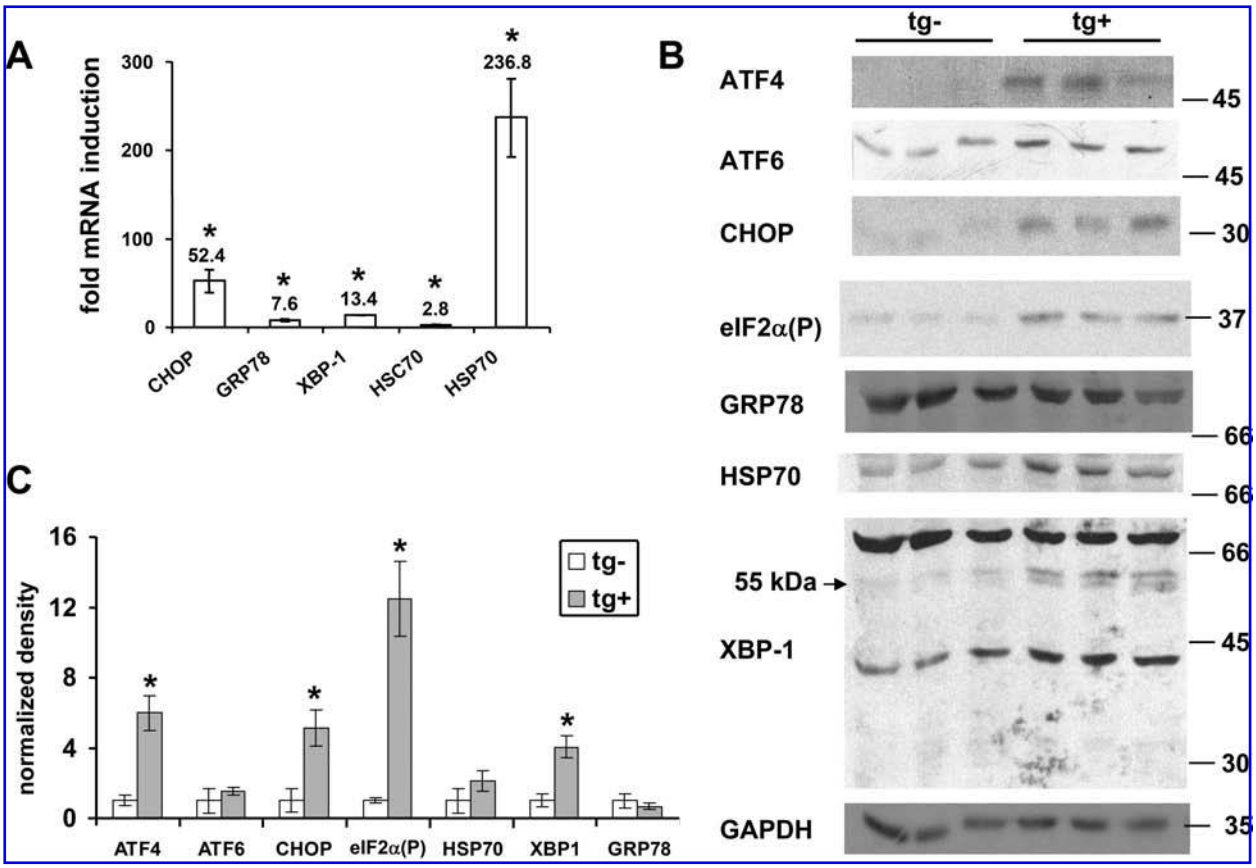

FIG. 6. Cellular stress responses in thapsigargin-treated neuroblastoma cells. (**A**) RT-PCR of stress gene induction after 2 m*M* thapsigargin (tg) for 3 h. *$p < 0.05$ by using one-tailed Student's *t* test for each PCR reaction, compared with untreated cells. (**B**) Western detection of protein markers of the UPR and HSR in untreated (tg-) and tg-treated (tg+) neuroblastoma cells after 2 m*M* tg for 3 h. (**C**) Densitometry for Westerns shown in **B**, normalized to levels of GAPDH for each lane. Graph for XBP-1 is the density of the 55-kDa translation product, shown by the *arrow* in **B**. *$p < 0.05$ by using one-tailed Student's *t* test.

higher in tg-treated cells than at any time point in reperfused CA1. Transcription of *grp78* increased sevenfold in the cells. It is relevant to note that, where quantitatively similar increases occurred between brain and cultured cells, these occurred in 3 h in tg-treated cells, but required 8–30 h to reach equivalent levels in the reperfused brain, and only then, in a regionally specific manner.

Western blots of UPR and HSR markers are shown in Fig. 6B, and the respective scanning densitometry is shown in Fig. 6C. Sixfold, fivefold, 12-fold, and fourfold increases were found in ATF4, CHOP, eIF2α(P), and 55-kDa XBP-1, respectively, after tg treatment. Although the amount of 50-kDa ATF6 increased about twofold, this did not clear statistically, and significant signal was found in untreated cells. Levels of GRP78 did not change, likely because of the eIF2α(P)-mediated translation block. GAPDH, used as a normalizer, did not change. Despite the very large increase in *hsp70* transcription, only a twofold increase in HSP70 protein occurred during the 3 h of tg treatment, consistent with a previous report of tg-treated primary neurons (32). Thus, unlike the reperfused brain, whose main stress-protein translation product was HSP70, the tg-treated cells showed low levels of HSP70, but the expected increases in both UPR-induced mRNAs and proteins. Comparison of the *in vivo* brain data with the tg-treated cells indicates that substantial differences in stress gene and protein expression distinguish these conditions.

DISCUSSION

We previously evaluated the UPR during early reperfusion after cardiac arrest–induced global brain ischemia and observed activation of PERK, modification of IRE1 without an accompanying processing of *xbp-1* mRNA, and no activation of ATF6 (21). We concluded that either PERK was activated independent of the UPR, or that some mechanism(s) interfered with pathways downstream of IRE1 and ATF6. In the present study, we extended our assessment of the UPR to 42-h reperfusion by using 2VO/HT ischemia, and additionally evaluated markers of the HSR. We showed that, even with longer reperfusion durations, generally a muted UPR-transcriptional response is confined only to vulnerable CA1, undetectable UPR translation products, and a very large expression of the HSR. These results, in combination with others in the literature, indicate that the cytoplasmic stress response predominates in the reperfused brain compared with the ER stress response.

Early reperfusion

By using 2VO/HT ischemia in the present study, we observed a fivefold increase in eIF2α(P) at 10-min reperfusion, substantially less than the ~12-fold increase observed in hippocampus at this same time point after cardiac arrest and resuscitation (21). The relatively lower levels of eIF2α(P) suggest that the 2VO/HT model induced less ER stress, and hence PERK activation, than the cardiac-arrest model. Nonetheless, DND occurred in the 2VO/HT model (see Fig. 1). We previously argued that eIF2α phosphorylation does not correlate with selective vulnerability (5, 6), and this conclusion is supported by the present result.

Changes in UPR-induced mRNAs

Regional differences were observed with *xbp-1*, *chop,* and *grp78* induction. Only *xbp-1* was induced in CA3. CA1, conversely, showed 12-fold, 10-fold, and fourfold inductions of *chop, xbp-1*, and *grp78*, respectively, although changes in *grp78* did not clear statistically. These data indicate that the ER stress response was stronger in CA1 than in CA3.

The magnitudes of mRNA changes we observed were generally consistent with other studies. Increased *grp78* during reperfusion has been reported (27, 44). Tajiri *et al*. noted a marked induction in whole hippocampus of *xbp-1*, and showed fivefold and twofold increases in *chop* and *grp78*, respectively, at 12-h reperfusion after 15-min BCAO in mice (43). Paschen *et al*. (35) showed an approximate sixfold increase in *chop* transcription in whole hippocampus at 8-h reperfusion with 10-min four-vessel occlusion (35) and showed twofold increases in both *chop* and *grp78* at 6 h after 60 min of focal cerebral ischemia (34), both in rat.

It is significant to note about these results: (a) the relatively small magnitude of the respective mRNA inductions, and (b) the long delay in induction compared with dedicated ER stress induction in culture systems. When we induced ER stress with tg in NB104 cells, *chop* and *grp78* were induced 50-fold and sevenfold within 3 h of treatment (see Fig. 6). Within a similar 3-h window, Mengesdorf *et al*. (32) also observed 20-fold and 15-fold increases in *chop* and *grp78* mRNAs after tg treatment of primary neuronal cultures (32).

We used induction of *xbp-1* mRNA as a marker of UPR-induced transcription (46), to assess the downstream functional consequences of ER stress at later reperfusion. We did not measure the processing of *xbp-1*, which is a surrogate marker of IRE1 activation (3, 22) and a proximal event in the UPR. We previously were unable to show evidence for processing of a significant percentage of *xbp-1* mRNA during early reperfusion (21), consistent with the very small fraction of processed *xbp-1* reported by Tajiri *et al.* (43). However, by using a different assay, Paschen *et al*. reported significant *xbp-1* processing after early reperfusion (34). One possible explanation for this discrepancy is that the assay used in (34) does not provide the percentage of *xbp-1* in the processed form, as do the assays used in (21) and (43), but measures the relative increase in the processed form. If the amount of processed *xbp-1* in controls is very small, this might lead to large relative increases, even if only representing a fraction of the total *xbp-1* mRNA.

Changes in UPR-induced proteins

Here we assessed ATF4, ATF6, CHOP, GRP78, and XBP-1. Despite our ability to detect these proteins in tg-treated NB104 cells (see Fig. 6), we could not detect ATF4 (see Fig. 2), the 50-kDa active form of ATF6 (not shown), CHOP (see Fig. 2), or the 55-kDa active form of XBP-1 (see Fig. 4B) at any time in the reperfused homogenates of either CA1 or CA3. General disagreement exists in the literature about the expression of these proteins, which is a particularly crucial issue to resolve, because these proteins are responsible for mediating the downstream functions of the UPR.

Hayashi *et al*. (12), with the same model as used here, showed increases in proteins of 26 and 50 kDa that they identified as

ATF4 and CHOP, respectively (12). However, the rat ATF4 (Accession NM 024403) and CHOP (Accession U36994) cDNA sequences predict proteins of molecular mass of ~43 kDa and 29 kDa, respectively. We detected ATF4 and CHOP as migrating at ~48 and 30 kDa, respectively, in tg-treated NB104 cells (see Fig. 6). Tajiri *et al*. (43) also reported increased CHOP by immunohistochemistry but did not validate this observation with Western blot (43). Because of the critical role CHOP plays in cell-death induction after the UPR (30), it is critical to resolve these apparent conflicts.

Although Paschen *et al*. (34) reported detection of 55-kDa XBP-1 after focal, but not global ischemia (34), we did not detect 55-kDa XBP-1 at any time in our samples, again, despite the ability to detect the protein in tg-treated NB104 cells. At high protein concentrations, we detected low levels of the 30-kDa XBP-1 in CA1 at later reperfusion (see Fig. 4B). Accumulation of the 30-kDa form of XBP-1 is consistent with the increase in *xbp-1*, but suggests that processing of the *xbp-1* mRNA did not occur. As the 55-kDa form of XBP-1 is the functional end point of the IRE1 pathway (3, 22), our data suggest that this pathway is nonfunctional during reperfusion. It is possible that an UPR-independent mechanism of *xbp-1* transcriptional upregulation was induced by I/R (*e.g*., as in 47), particularly as *xbp-1* induction did not distinguish CA1 and CA3. It also bears mention that increased 30-kDa XBP-1 occurred at the same times as we detected significant HSP70 synthesis in CA1 (see Fig. 5), indicating that the translation block in CA1 at later reperfusion is not absolute in the present model.

Increased GRP78 protein has been reported to occur after focal ischemia (44) and after ischemic preconditioning (12), but was not observed by 4-h reperfusion after global I/R (9). We observed a continuous decline in levels of GRP78 in CA1. In CA3, the doubling of GRP78 protein at 18R was not accompanied by a change in *grp78* mRNA, and a decrease in GRP78 was seen after 18R. Although in principle a protective effect, validation of the *de novo* synthesis of GRP78 in CA3 will require *in vivo* radiolabeling and GRP78 immunoprecipitation. The lack of significant change in *grp78* mRNA, coupled with a decline in the protein levels, further indicates a muted UPR response in reperfused brain.

It is possible that the UPR-induced proteins were translated *de novo* but below our detection limits. However, Hayashi *et al.* (12) reported detection of these proteins in 5 μg of homogenate, and here we used 50 μg per gel lane. Additionally, when we loaded 130 μg per lane, we still could not detect 50-kDa ATF6 and CHOP (data not shown), or 55-kDa XBP-1, but did detect the 30-kDa form of XBP-1 (see Fig. 4B). If CHOP or 55-kDa XBP-1 were present in 130 μg homogenate but at undetectable levels, then it would be expected that their activities would be correspondingly low. Thus, we conclude that DND occurred in CA1 in the present model in the either the absence or in the presence of undetectable levels of CHOP.

Does brain ischemia and reperfusion activate the UPR?

The UPR is currently defined by simultaneous activation of PERK, IRE1, and ATF6 after ER stress, and their subsequent downstream effects *via* increased transcription and translation of products such as ATF4, CHOP, GADD34, and XBP-1, leading to either cell survival or cell death (1). After brain I/R, unambiguous evidence exists for PERK activation and eIF2α phosphorylation [see Fig. 2 and (20, 21, 13)], conflicting evidence of the extent of IRE1 activation (discussed earlier), and no evidence for ATF6 activation [the present study and (21)]. Conflicting evidence also exists for downstream transcriptional and translational effects. There is generally a delayed and muted expression of UPR-induced mRNAs, and subsequent protein expression has been difficult to establish. Some of these differences may arise from differences in ischemia models and species. The persistent translation block associated with vulnerable neurons may contribute substantially to muting UPR expression (36). That this ambiguity exists strongly suggests that brain I/R either does not trigger a classical UPR or somehow interferes with its expression.

Given the intense and rapid activation of PERK, it is possible that the pathways activated by I/R in brain more resemble the ISR than the UPR. The ISR results in increased translation of ATF4 *via* internal reinitiation (29), which itself can induce *chop* (10) and *gadd34* transcription (2), whereas the ISR is not specific for increasing ER-specific proteins such as GRP78 or XBP-1. GADD34 is an eIF2α(P) phosphatase–targeting subunit (33) Thus, activation of PERK phosphorylation of eIF2α (13, 20, 21) increased GADD34 mRNA (18, 35) and protein (9, 17, 45), and although we could not confirm it here, the reported increases in ATF4 (12) and CHOP (12, 43) are more consistent with activation of the ISR.

Magnitudes of neuronal stress responses

We showed here, consistent with findings known since the 1980s (reviewed in 38, 41), a very large and robust expression of the mRNA and protein for HSP70 in the postischemic brain. Even the largest relative increase in ER stress–induced transcription was an order of magnitude less than the relative induction of HSP70 mRNA in the present study. This large difference in magnitude between the HSR and UPR/ISR is expected to be of pathophysiologic significance.

In a study of the quantitative expression of the UPR, Shang and Lehrman (40) showed that the amount of mRNA induced after ER stress did not correlate with the degree of activation of ATF6 or IRE1 in response to the same stress. However, although not correlated to ATF6/IRE1 activation levels, the amount of mRNA induced was proportional to the type and degree of ER stress. This result is relevant to assessment of stress responses after brain I/R because it allows us to appreciate that the degree of stress-gene induction, although not directly related to the degree of effector activation, is correlated with the degree of the upstream stress itself.

On this basis, the very large increase in *hsp70* mRNA, compared with any of the ER stress–induced mRNAs, indicates that cytoplasmic stress predominated over ER stress in the reperfused brain. However, this assumption is tempered by the consideration that the degree of transcriptional induction is also a function of the relevant promoter. The technique used here to measure mRNA changes provided the relative increase over the control baseline condition, but did not provide information as to what percentage of the total possible increases our results represented. It is possible, for example, that, proportionately

speaking, we observed a relatively small increase in the HSR and a relatively large increase in ER stress–related transcription.

Conversely, one must consider the functional consequences associated with the relative increases in mRNAs observed in the present study. At their respective peaks, 12-fold and 400-fold increases were noted in *chop* and *hsp70* mRNAs in reperfused CA1. Functionally, in CA1, HSP70 was eventually translated, whereas we could not detect CHOP protein at any point. On this basis, then, our results suggest that factors related to the HSR outweighed those related to ER stress, which in turn suggests that damage to the cytoplasmic compartment, as opposed to the ER, is of greater functional significance in the postischemic brain.

The very large increase in the HSR is consistent with the rapid accumulation of ubiquinated proteins and misfolded protein aggregates in the cytoplasm of postischemic neurons. Ubiquinated protein accumulation is reversible in resistant areas such as CA3, being cleared after 24-h reperfusion, but protein aggregates are irreversible in vulnerable CA1 (15, 16, 24, 48). Our present results, showing a lag of about 24 h in the translation of HSP70, is consistent with the interpretation that it is the delayed translation of HSP70, despite very high levels of transcripts in the cells, that may play a crucial role in the selective death of CA1 neurons. Conversely, despite changes in ER stress–related mRNAs, we could not detect increases in key functional proteins (CHOP, 55-kDa XBP-1, 50-kDa ATF6) in postischemic brain.

CONCLUSION

We extended the study of the UPR after brain I/R by evaluating it specifically in microdissected CA1 and CA3 out to 42-h reperfusion, just 1 day before CA1 cells die by DND. Additionally, we evaluated makers of the UPR alongside those of the HSR to gauge the relative degree of activation of both stress responses. Our main conclusions are: (a) if brain I/R does trigger a classic UPR, then its expression is muted; (b) based on effector activation and downstream products, the ER stress response in I/R brain more resembles the IRS than the UPR; and (c) that the magnitude of the HSR is much greater than ER-stress pathways in terms of functional downstream products. Thus, whereas I/R causes multiple upstream damage mechanisms, the present results suggest that further investigations into why postischemic neurons express a relatively strong HSR, and why this is differentially expressed between vulnerable and resistant neurons, may be of importance for developing effective therapies to halt postischemic brain damage.

ACKNOWLEDGMENTS

We thank Drs. Heather Harding and David Ron for supplying XBP-1 antiserum. We thank Jennifer Gutwald, M.D., for her help with the Western blots. We thank Dr. Heather Montie for her suggestions for GAPDH and general Western detection. This work was sponsored by NIH grant NS044100 (D.J.D.).

ABBREVIATIONS

ATF, activating transcription factor; CA, cornu Ammonis (Ammon's horn); CHOP, cAMP response element–binding protein (CREB) enhancer–binding protein (CEBP) homology protein; eIF2α, α subunit of eukaryotic initiation factor 2; ISR, integrated stress response; GAPDH, glyceraldehyde phosphate dehydrogenase; GRP78, glucose-regulated protein 78 kDa; HSC70, constitutive 70-kDa heat-shock protein; HSP70, inducible heat-shock protein 70 kDa; HSR, heat-shock response; I/R, ischemia and reperfusion; UPR, unfolded protein response; XBP-1, x-box–binding protein.

REFERENCES

1. Bernales S, Papa FR, and Walter P. Intracellular signaling by the unfolded protein response. *Annu Rev Cell Dev Biol* 22: 487–508, 2006.
2. Blais JD, Filipenko V, Bi M, Harding HP, Ron D, Koumenis C, Wouters BG, and Bell JC. Activating transcription factor 4 is translationally regulated by hypoxic stress. *Mol Cell Biol* 24: 7469–7482, 2004.
3. Calfon M, Zeng H, Urano F, Till JH, Hubbard SR, Harding HP, Clark SG, and Ron D. IRE1 couples endoplasmic reticulum load to secretory capacity by processing the XBP-1 mRNA. *Nature* 415: 92–96, 2002.
4. Cardozo AK, Ortis F, Storling J, Feng YM, Rasschaert J, Tonnesen M, Van Eylen F, Mandrup-Poulsen T, Herchuelz A, and Eizirik DL. Cytokines downregulate the sarcoendoplasmic reticulum pump Ca^{2+} ATPase 2b and deplete endoplasmic reticulum Ca^{2+}, leading to induction of endoplasmic reticulum stress in pancreatic beta-cells. *Diabetes* 54: 452–461, 2005.
5. DeGracia DJ. Acute and persistent protein synthesis inhibition following cerebral reperfusion. *J Neurosci Res* 77: 771–776, 2004
6. DeGracia DJ and Hu BR. Irreversible translation arrest in the reperfused brain. *J Cereb Blood Flow Metab* Epub ahead of print: PMID: 16926841, 2006.
7. DeGracia DJ and Montie HL. Cerebral ischemia and the unfolded protein response. *J Neurochem* 91: 1–8, 2004
8. DeGracia DJ, Rudolph J, Roberts G, and Wang J. Convergence of stress granules and protein aggregates following ischemia. *Neuroscience* 2007. doi:10.1016/j.*neuroscience*.2007.01. 050.
9. Garcia L, Burda J, Hrehorovska M, Burda R, Martin ME, and Salinas M. Ischaemic preconditioning in the rat brain: effect on the activity of several initiation factors, Akt and extracellular signal-regulated protein kinase phosphorylation, and GRP78 and GADD34 expression. *J Neurochem* 88: 136–147, 2004.
10. Harding HP, Novoa I, Zhang Y, Zeng H, Wek R, Schapira M, and Ron D. Regulated translation initiation controls stress-induced gene expression in mammalian cells. *Mol Cell* 6: 1099–1108, 2000.
11. Hayashi T, Saito A, Okuno S, Ferrand-Drake M, and Chan PH. Induction of GRP78 by ischemic preconditioning reduces endoplasmic reticulum stress and prevents delayed neuronal cell death. *J Cereb Blood Flow Metab* 23: 949–961, 2003.
12. Hayashi T, Saito A, Okuno S, Ferrand-Drake M, Dodd RL, and Chan PH. Damage to the endoplasmic reticulum and activation of apoptotic machinery by oxidative stress in ischemic neurons. *J Cereb Blood Flow Metab* 25: 41–53, 2005.
13. Hayashi T, Saito A, Okuno S, Ferrand-Drake M, Dodd RL, Nishi T, Maier CM, Kinouchi H, and Chan PH. Oxidative damage to the endoplasmic reticulum is implicated in ischemic neuronal cell death. *J Cereb Blood Flow Metab* 23: 1117–1128, 2003.
14. Hossmann KA. Disturbances of cerebral protein synthesis and ischemic cell death. *Prog Brain Res* 96: 161–177, 1993.
15. Hu BR, Janelidze S, Ginsberg MD, Busto R, Perez-Pinzon M, Sick TJ, Siesjo BK, and Liu CL. Protein aggregation after focal brain ischemia and reperfusion. *J Cereb Blood Flow Metab* 21: 865–875, 2001.

16. Hu BR, Martone ME, Jones YZ, and Liu CL. Protein aggregation after transient cerebral ischemia. *J Neurosci* 20: 3191–3199, 2000.
17. Imai H, Harland J, McCulloch J, Graham DI, Brown SM, and Macrae IM. Specific expression of the cell cycle regulation proteins, GADD34 and PCNA, in the peri-infarct zone after focal cerebral ischaemia in the rat. *Eur J Neurosci* 15: 1929–1936, 2002.
18. Jin K, Mao XO, Eshoo MW, Nagayama T, Minami M, Simon RP, and Greenberg DA. Microarray analysis of hippocampal gene expression in global cerebral ischemia. *Ann Neurol* 50: 93–103, 2001.
19. Kaufman RJ. Stress signaling from the lumen of the endoplasmic reticulum: coordination of gene transcriptional and translational controls. *Genes Dev* 13: 1211–1233, 1999
20. Kumar R, Azam S, Sullivan JM, Owen C, Cavener DR, Zhang P, Ron D, Harding HP, Chen JJ, Han A, White BC, Krause GS, and DeGracia DJ. Brain ischemia and reperfusion activates the eukaryotic initiation factor 2α kinase, PERK. *J Neurochem* 77: 1418–1421, 2001.
21. Kumar R, Krause GS, Yoshida H, Mori K, and DeGracia DJ. Dysfunction of the unfolded protein response during global brain ischemia and reperfusion. *J Cereb Blood Flow Metab* 23: 462–471, 2003.
22. Lee K, Tirasophon W, Shen X, Michalak M, Prywes R, Okada T, Yoshida H, Mori K, and Kaufman RJ. IRE1-mediated unconventional mRNA splicing and S2P-mediated ATF6 cleavage merge to regulate XBP1 in signaling the unfolded protein response. *Genes Dev* 16: 452–466, 2002.
23. Liu C, Truttner J, Chen S, Dietrich D, Bramlett H, and Hu BR. Cytoplasmic, mitochondrial or ER stress response after transient cerebral ischemia [Abstract]. *J Cereb Blood Flow Metab* 25: S428, 2005.
24. Liu CL, Ge P, Zhang F, and Hu BR. Co-translational protein aggregation after transient cerebral ischemia. *Neuroscience* 134: 1273–1284, 2005.
25. Livak KJ and Schmittgen TD. Analysis of relative gene expression data using real-time quantitative PCR and the $2^{\Delta\Delta CT}$ method. *Methods* 25: 402–408, 2001.
26. Longo FM, Wang S, Narasimhan P, Zhang JS, Chen J, Massa SM, and Sharp FJ. cDNA cloning and expression of stress-inducible rat hsp70 in normal and injured rat brain. *J Neurosci Res* 36: 325–335, 1993.
27. Lowenstein DH, Gwinn RP, Seren MS, Simon RP, and McIntosh TK. Increased expression of mRNA encoding calbindin-D28K, the glucose-regulated proteins, or the 72 kDa heat-shock protein in three models of acute CNS injury. *Brain Res Mol Brain Res* 22: 299–308, 1994.
28. Lu L, Roberts GG, Oszust C, and Hudson AP. The YJR127C/ZMS1 gene product is involved in glycerol-based respiratory growth of the yeast *Saccharomyces cerevisiae*. *Curr Genet* 48: 235–246, 2005.
29. Lu PD, Harding HP, and Ron D. Translation reinitiation at alternative open reading frames regulates gene expression in an integrated stress response. *J Cell Biol* 167: 27–33, 2004.
30. Marciniak SJ, Yun CY, Oyadomari S, Novoa I, Zhang Y, Jungreis R, Nagata K, Harding HP, and Ron D. CHOP induces death by promoting protein synthesis and oxidation in the stressed endoplasmic reticulum. *Genes Dev* 18: 3066–3077, 2004.
31. McEntee CM and Hudson AP. Preparation of RNA from unspheroplasted yeast cells (*Saccharomyces cerevisiae*). *Anal Biochem* 176: 303–306, 1989.
32. Mengesdorf T, Althausen S, Oberndorfer I, and Paschen W. Response of neurons to an irreversible inhibition of endoplasmic reticulum Ca(2+)-ATPase: relationship between global protein synthesis and expression and translation of individual genes. *Biochem J* 15: 805–812, 2001.
33. Novoa I, Zeng H, Harding HP, and Ron D. Feedback inhibition of the unfolded protein response by GADD34-mediated dephosphorylation of eIF2α. *J Cell Biol* 153: 1011–1122, 2001.
34. Paschen W, Aufenberg C, Hotop S, and Mengesdorf T. Transient cerebral ischemia activates processing of *xbp1* messenger RNA indicative of endoplasmic reticulum stress. *J Cereb Blood Flow Metab* 23: 449–461, 2003.
35. Paschen W, Gissel C, Linden T, Althausen S, and Doutheil J. Activation of gadd153 expression through transient cerebral ischemia: evidence that ischemia causes endoplasmic reticulum dysfunction. *Brain Res Mol Brain Res* 60: 115–122, 1998.
36. Paschen W. Shutdown of translation: lethal or protective? Unfolded protein response versus apoptosis. *J Cereb Blood Flow Metab* 23: 77377–77379, 2003.
37. Paxinos G and Watson C. *The rat brain in stereotaxic coordinates*. New York: Academic Press, 1998.
38. Planas AM, Soriano MA, Estrada A, Sanz O, Martin F, and Ferrer I. The heat shock stress response after brain lesions: induction of 72 kDa heat shock protein (cell types involved, axonal transport, transcriptional regulation) and protein synthesis inhibition. *Prog Neurobiol* 51: 607–636, 1997.
39. Ron D and Harding HP. eIF2α phosphorylation in cellular stress responses and disease. In: *Translational control in biology and medicine,* edited by Matthews MB, Sonnenberg N, and Hershey JWB. Woodbury, New York: Cold Spring Harbor Laboratory Press, 2006, pp. 345–368.
40. Shang J and Lehrman MA. Discordance of UPR signaling by ATF6 and Ire1p-XBP1 with levels of target transcripts. *Biochem Biophys Res Commun* 317: 390–396, 2004.
41. Sharp FR, Massa SM, and Swanson RA. Heat-shock protein protection. *Trends Neurosci* 22: 97–99, 1999.
42. Smith ML, Bendek G, Dahlgren N, Rosen I, Wieloch T, and Siesjo BK. Models for studying long-term recovery following forebrain ischemia in the rat. 2. A 2-vessel occlusion model. *Acta Neurol Scand* 69: 385–401, 1984.
43. Tajiri S, Oyadomari S, Yano S, Morioka M, Gotoh T, Hamada JI, Ushio Y, and Mori M. Ischemia-induced neuronal cell death is mediated by the endoplasmic reticulum stress pathway involving CHOP. *Cell Death Differ* 11: 403–415, 2004.
44. Wang P, Longo FM, Chen J, Butman M, Graham SH, Haglid KG, and Sharp FR. Induction of glucose regulated protein (grp78) and inducible heat shock protein (hsp70) mRNAs in rat brain after kainic acid seizures and focal ischemia. *Neurochem Int* 23: 575–582,1993.
45. White F, McCaig D, Brown SM, Graham DI, Harland J, and Macrae IM. Up-regulation of a growth arrest and DNA damage protein (GADD34) in the ischaemic human brain: implications for protein synthesis regulation and DNA repair. *Neuropathol Appl Neurobiol* 30: 683–691, 2004.
46. Yoshida H, Okada T, Haze K, Yanagi H, Yura T, Negishi M, and Mori K. ATF6 activated by proteolysis binds in the presence of NF-Y (CBF) directly to the cis-acting element responsible for the mammalian unfolded protein response. *Mol Cell Biol* 20: 6755–6767, 2000.
47. Zambelli A, Mongiardini E, Villegas SN, Carri NG, Boot-Handford RP, and Wallis GA. Transcription factor XBP-1 is expressed during osteoblast differentiation and is transcriptionally regulated by parathyroid hormone (PTH). *Cell Biol Int* 29: 647–653, 2005.
48. Zhang F, Liu CL, and Hu BR. Irreversible aggregation of protein synthesis machinery after focal brain ischemia. *J Neurochem* 98: 102–112, 2006.

Address reprint requests to:
Dr. D. J. DeGracia
Department of Physiology
Wayne State University
4116 Scott Hall
540 East Canfield Ave.
Detroit, MI

E-mail: ddegraci@med.wayne.edu

Date of first submission to ARS Central, June 17, 2007; date of acceptance, June 23, 2007.

This article has been cited by:

1. Juan Bin, Qian Wang, Ye-Ye Zhuo, Jiang-Ping Xu, Han-Ting Zhang. 2012. Piperphentonamine (PPTA) attenuated cerebral ischemia-induced memory deficits via neuroprotection associated with anti-apoptotic activity. *Metabolic Brain Disease* . [CrossRef]
2. J.T. Jamison, J.J. Szymanski, D.J. DeGracia. 2011. Organelles do not colocalize with mRNA granules in post-ischemic neurons. *Neuroscience* **199**, 394-400. [CrossRef]
3. Clara Penas , Arán Pascual-Font , Renzo Mancuso , Joaquim Forés , Caty Casas , Xavier Navarro . 2011. Sigma Receptor Agonist 2-(4-Morpholinethyl)1 Phenylcyclohexanecarboxylate (Pre084) Increases GDNF and BiP Expression and Promotes Neuroprotection after Root Avulsion Injury. *Journal of Neurotrauma* **28**:5, 831-840. [Abstract] [Full Text HTML] [Full Text PDF] [Full Text PDF with Links]
4. Jeffrey J. Szymanski, Jill T. Jamison, Donald J. DeGracia. 2011. Texture analysis of poly-adenylated mRNA staining following global brain ischemia and reperfusion. *Computer Methods and Programs in Biomedicine* . [CrossRef]
5. Katie Facecchia, Lee-Anne Fochesato, Sidhartha D. Ray, Sidney J. Stohs, Siyaram Pandey. 2011. Oxidative Toxicity in Neurodegenerative Diseases: Role of Mitochondrial Dysfunction and Therapeutic Strategies. *Journal of Toxicology* **2011**, 1-12. [CrossRef]
6. R. Anne Stetler, Yu Gan, Wenting Zhang, Anthony K. Liou, Yanqin Gao, Guodong Cao, Jun Chen. 2010. Heat shock proteins: Cellular and molecular mechanisms in the central nervous system. *Progress in Neurobiology* **92**:2, 184-211. [CrossRef]
7. Xiao-Cai Sun, Xiao-Hui Xian, Wen-Bin Li, Li Li, Cai-Zhen Yan, Qing-Jun Li, Min Zhang. 2010. Activation of p38 MAPK participates in brain ischemic tolerance induced by limb ischemic preconditioning by up-regulating HSP 70. *Experimental Neurology* **224**:2, 347-355. [CrossRef]
8. Miklós Csala , Éva Margittai , Gábor Bánhegyi . 2010. Redox Control of Endoplasmic Reticulum Function. *Antioxidants & Redox Signaling* **13**:1, 77-108. [Abstract] [Full Text HTML] [Full Text PDF] [Full Text PDF with Links]
9. Seema Yousuf, Fahim Atif, Muzamil Ahmad, Nasrul Hoda, Tauheed Ishrat, Badruzaman Khan, Fakhrul Islam. 2009. Resveratrol exerts its neuroprotective effect by modulating mitochondrial dysfunctions and associated cell death during cerebral ischemia. *Brain Research* **1250**, 242-253. [CrossRef]
10. Gábor Bánhegyi, József Mandl, Miklós Csala. 2008. Redox-based endoplasmic reticulum dysfunction in neurological diseases. *Journal of Neurochemistry* **107**:1, 20-34. [CrossRef]
11. Donald J. DeGracia, Jill T. Jamison, Jeffrey J. Szymanski, Monique K. Lewis. 2008. Translation arrest and ribonomics in post-ischemic brain: layers and layers of players. *Journal of Neurochemistry* **106**:6, 2288-2301. [CrossRef]
12. Y. Oida, H. Izuta, A. Oyagi, M. Shimazawa, T. Kudo, K. Imaizumi, H. Hara. 2008. Induction of BiP, an ER-resident protein, prevents the neuronal death induced by transient forebrain ischemia in gerbil. *Brain Research* **1208**, 217-224. [CrossRef]
13. Martin Schröder , Kenji Kohno . 2007. Recent Advances in Understanding the Unfolded Protein Response. *Antioxidants & Redox Signaling* **9**:12, 2241-2244. [Citation] [Full Text PDF] [Full Text PDF with Links]
14. D.J. DeGracia, J. Rudolph, G.G. Roberts, J.A. Rafols, J. Wang. 2007. Convergence of stress granules and protein aggregates in hippocampal cornu ammonis 1 at later reperfusion following global brain ischemia. *Neuroscience* **146**:2, 562-572. [CrossRef]